Reflex Control of the Pisa/IIT SoftHand during Object Slippage

Arash Ajoudani[1], Elif Hocaoglu[1], Alessandro Altobelli[1], Matteo Rossi[1,2], Edoardo Battaglia[2], Nikos Tsagarakis[1], and Antonio Bicchi[1,2]

***Abstract*— In this work, to guarantee the Pisa/IIT SoftHand's grasp robustness against slippage, three reflex control modes, namely Current, Pose and Impedance, are implemented and experimentally evaluated. Towards this objective, ThimbleSense fingertip sensors are designed and integrated into the thumb and middle fingers of the SoftHand for real-time detection and control of the slippage. Current reflex regulates the restoring grasp forces of the hand by modulating the motor's current profile according to an update law. Pose and Impedance reflex modes instead replicate this behaviour by implementing an impedance control scheme. The difference between the two latter is that the stiffness gain in Impedance reflex mode is being varied in addition to the hand pose, as a function of the slippage on the fingertips. Experimental setup also includes a seven degrees-of-freedom robotic arm to realize consistent trajectories (e.g. lifting) among three control modes for the sake of comparison. Different test objects are considered to evaluate the efficacy of the proposed reflex modes in our experimental setup. Results suggest that task-appropriate restoring forces can be achieved using Impedance reflex due to its capability in demonstrating instantaneous and rather smooth reflexive behaviour during slippage. Preliminary experiments on five healthy human subjects provide evidence on the similarity of the control concepts exploited by the humans and the one realized by the Impedance reflex, highlighting its potential in prosthetic applications.**

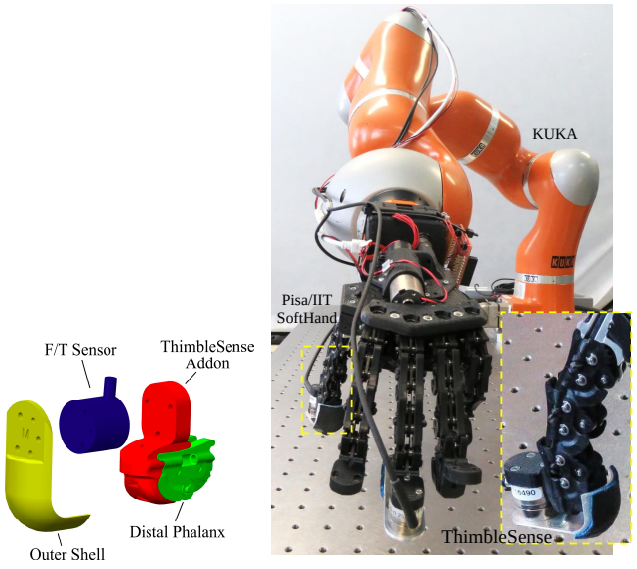

Fig. 1: a) ThimbleSense addon for the Pisa/IIT SoftHand, and b) two ThimbleSenses attached to the thumb and middle fingers of the Pisa/IIT SoftHand. The hand is mounted on the end-effector of the KUKA lightweight robotic arm.

I. Introduction

The central nervous system of human steadily regulates the grip forces exerted by the hand in order to avoid slippage of the object out of the grasp with a safety margin of 10 – 40% [1]. At the very beginning of the grasp, gripping force is generated depending on the estimation of the load and altered based on the feedback provided by the hand receptors. Such behaviour is dominated by the spinal cord and recognized as reflex control.

The most basic way to achieve a similar performance in prosthetic or robotic hands is to exert high level grip forces to prevent slippage of the grasped object. This method, however, poses some difficulties while dealing with fragile or deformable objects. As a consequence, toward the twofold purpose of improving the grasp robustness against slippage and avoiding the generation of unnecessarily high interaction forces, some robotic/prosthetic hands replicate a human-like reflexive behaviour and regulate grip forces once a slippage is detected [2], [3].

Slip detection has been realized with the aid of various techniques, e.g. vibration, optical tracking, pressure, and force vector control [4]–[8]. Based on the studies in neurophysiology, humans perceive slide of objects with the occurrence of firing activity generated in Pacinian corpuscles, which are nerve endings in the skin, sensitive to high frequency vibrations [9]. In the light of this information, some researchers focused on the vibration based techniques to prevent object slippage during the grasp. Cutkosky *et al.* proposed a method for incipient slippage detection by sensing vibrations generated by the spread of slip zone inside the contact area while the tangential force increases [4]. A couple of accelerometers were placed near and on top of the contact region to detect vibrations due to the slippage and noise, respectively. As a commercial example, BioTac fingertip sensors that are capable of sensing force, vibration and temperature, detect slippage by means of vibration. Results of this study suggest that the high-frequency spectral power from 30-200 Hz can be a reliable indicator of sliding [10]. Even though vibration based techniques are commonly used to warn the system for incipient slippage, they are not very robust in the presence of disturbances; in particular,

[1]Department of Advanced Robotics, Istituto Italiano di Tecnologia, Via Morego 30, 16163, Genova, Italy. [2]Centro di Ricerca E. Piaggio, Universita di Pisa, Pisa, Italy. Emails: {arash.ajoudani, elif.hocaoglu, alessandro.altobelli, matteo.rossi, nikos.tsagarakis}@iit.it, {e.battaglia, bicchi}@centropiaggio.unipi.it

Authors would like to thank Michele Canepa and Nicolo Boccardo for their support on the design of the SoftHand controller. This work is supported in part by the (H2020-EU.2.1.1.5) project "Soft-bodied intelligence for Manipulation (SOMA)", and by the EU FP7 project (601165), "WEARable HAPtics for Humans and Robots (WEARHAP)".

unexpected changes during loading or manipulation phases, may produce undesired vibrations that can compromise the efficacy of the slip detection [4].

Optical sensing has also been employed in closed loop control systems to regulate the grasping force of hand prostheses by detecting the amount of object slippage. For instance, authors in [5] utilized an optical tracking sensor together with an i-Limb prosthetic hand [3]. Experimental results showed the efficacy of the optical tracking sensor while reducing the slippage of the cylindrical object under different loading conditions. Due to its size, the sensor was placed on the palm of the hand prosthesis; in such a system the slip detection feature can only be used if the objects to be grasp are big enough and therefore can be grasped by the fingers while remaining in the visual field of the sensor. Besides, it is known that such a system does not work well for glossy and smooth surfaces.

Other avenues of research seek for appropriate reflexive strategies once the slippage is detected. In particular, Mouri *et al.* proposed a human-like reflexive control strategy while grasping objects with unknown shapes. In this study, to control the 16 DoF anthropomorphic hand, the grasp was divided in two sub-phases: grasping and withholding. During the grasping phase, the hand was controlled with a velocity control if no contact was detected, and force control in the presence of a contact. During the withholding phase, force control was used and the Euclidean norm of the contact point velocity was added to the desired contact force to avoid slippage [11]. Authors in [12] use a prototype optical three axis tactile sensor for the analysis and detection of the normal and tangential forces in a two-finger robotic grasp. The rigid fingers' re-pushing velocity is controlled based on the object's classified stiffness to stabilize the grasp. In [2] an underactuated and myoelectric (EMG) controlled hand prosthesis equipped with the position and force sensors is exploited to realize successful grasps for different weight of objects with various grasp types (e.g. power and pinch grasp). To achieve this, three different control strategies based on the shared autonomy between the low-level and high-level (user intention) control were proposed. Results suggest that the incorporation of the human intention into the control loop increases the success rate of the grasping action. Alternatively, a research group [13] explored a useful relation between the reflexive responses of humans in various conditions and features of the measured EMG signals in order to functionalize hand prostheses against unexpected disturbances. The proposed technique, however, requires feature extraction analysis and decision algorithm to detect the grasp reflex time, which introduce more computational load to the system.

In this work, as a primary step towards the accomplishment of a reliable grasp in an underactuated anthropomorphic robotic/prosthetic hand, different reflex control strategies are implemented and experimentally evaluated. Given the adaptive and synergy-driven hand functionalities, the design of the hand reflex controller is inspired by the observations in human grasping experiments described in section II. In our

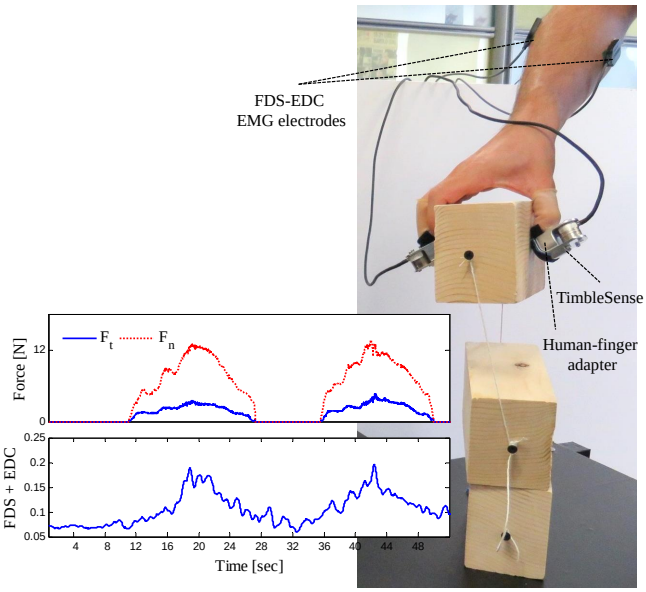

Fig. 2: Two ThimbeSenses are worn by the human while grasping the test object. The tangential (blue, solid) and normal (red, dotted) forces at the contact point of the thumb, and the summed EMG values of the FDS and EDC muscles of a typical experiment for two repetitions of a complete sequence (grasping, lifting and putting down the experimental object) are illustrated in the top and bottom plots, respectively.

setup (see Fig. 1), due to the limited space in the fingertip area, small and lightweight tactile sensors were required for real-time detection of the object slippage. To achieve this, a force-torque sensor based tactile sensory system is designed and integrated into the fingertips of the robotic hand for the estimation of the tangential and normal forces and torques at the corresponding point of contact.

II. Biomechanical Control Principles in Grasping: A Preliminary Study

Prior to the design of the robotic hand's reflex controller, a series of preliminary human grasping experiments were carried out to understand the underlying biomechanical principles that result in stable and reliable grasping of various objects[1]. Such principles can potentially be a source of inspiration to achieve an appropriate mechanical interface between the fingertips of the robotic hand and the object.

In our setup, human subjects wore two ThimbleSense tactile sensors on the index and thumb fingertips for real-time measurements of the grasping forces during the experiments (see Fig. 2). ThimbleSense [16] is a sensorized system that provides full-fledged measurement of force (normal and tangential at the contact point) and torque components, together with the location of contacts, and can be placed on fingertips for analysis of unconstrained grasping tasks. This is obtained by assembling a Force/Torque sensor (ATI Nano

[1]It is worth mentioning that even though several research groups investigated the feasibility of achieving a similar human-like grasping performance in robotic hands, only few studies consider the contribution of the mechanical impedance of the fingers in grasp robustness to disturbances such as slippage (e.g. see [14], [15]).

17) between an inner and an outer shell separated by a gap. Due to the rigid coupling between the sensor's outer shell and the human finger, meaningful information can still be transmitted to the fingertip receptors.

Due to the known geometry of the external support, it is possible to obtain the position of the contact centroid of the loading force, through the intrinsic tactile sensing algorithm defined by Bicchi et al. in [17]. More in general, given a surface S with an outward normal defined everywhere, and a distribution of compressive tractions applied on it, the contact centroid is defined as a point c such that a wrench exists and consists of a force directed into S applied to c and a pure torque about the contact normal. The intrinsic tactile sensing algorithm can be used to identify the contact centroid on a general surface, as long as it can be represented by a NURB (Non Uniform Rational B-Splines) parametrization: an application was provided in the Tactile Toolbox [18].

An object (Fig. 4, most left), which is consisted of three wooden blocks that are interconnected by strings, was designed to emulate sudden grasp force variations induced by the gravitational loading while lifting. Realization of a robust and reliable grasp while picking such an object requires that the grasping forces are appropriately regulated. In addition, similar objects with different surface properties (Fig. 4, three objects on the right) were taken into account to investigate the role of surface texture (friction properties) in grasp force modulations.

Five naive subjects participated in our experiments. Each subject was asked to pick the object naturally and place it back ten times, using only the thumb and index finger to perform the grasp. To minimize the effect of learning, objects were sorted in a random order. During the experiments, two surface electromyography (EMG) sensors collected the muscle activities of a dominant finger flexor/extensor antagonistic pair (FDS: Flexor Digitorum Superficialis and EDC: Extensor Digitorum Communis). Corresponding EMG signals were then processed (full rectified, filtered and normalized) for further analysis.

Typical results of the experiment with the interconnected three wooden blocks are illustrated in Fig 2. The tangential (blue, solid) and normal (red, dotted) forces at the contact point of the thumb, and the summed EMG values of the FDS and EDC muscles for two repetitions of a complete sequence (grasping, lifting and putting down the object) are illustrated in the top and the bottom plots, respectively. As observed in the plots, once a change in the gravitational loading of the object is detected, the normal forces are effectively regulated to achieve a reliable grasp[2]. Such interaction forces ensure the task execution and its robustness against disturbances (e.g. object slippage) that might be caused by sudden mass variations.

[2]As expected, when lifting the three objects that had the same weight and shape but different surface type, the normal force exerted was highly correlated with the surface type; in particular, the highest normal forces were exerted when lifting the object that had lowest surface friction and vice versa. In accordance with [1], it was found that the safety margin in the regulation of the normal forces was kept between 16% and 42%.

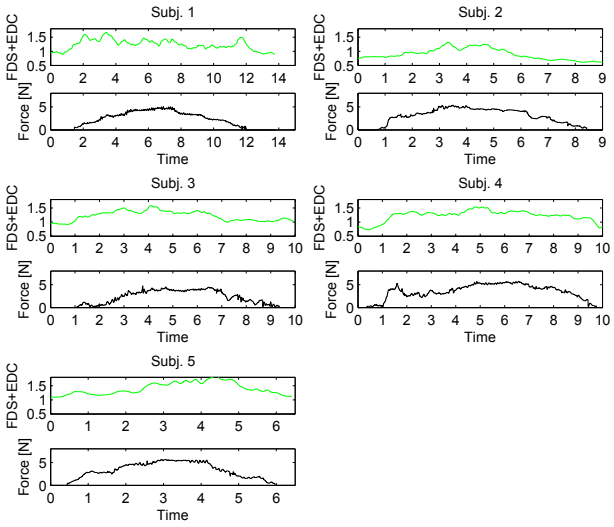

Fig. 3: Example of tangential forces and summed EMG values of the FDS and EDC muscles are plotted for the five subjects. These values are recorded during the grasp of the interconnected wooden blocks.

On the other hand, an increase in the FDS and EDC EMG signal amplitudes can be observed in correspondence of the lifting phase (see a similar trend for all subjects in Fig. 3). It is well-known that the increased activity of the antagonistic pair accounts for an increase in the grasp stiffness. Since the limb stiffness and pose can be regulated in a decoupled way in humans [19], simultaneous increase of the interaction forces as a consequence to the stiffening of the human fingers suggest that the virtual pose (equilibrium position, which is not measurable) of the finger is moved into the object. This is because, considering a simple and static formulation of the fingertip impedance, i.e. $F_n = k_n \Delta x_n$, with F_n, k_n and Δx_n being the normal component of the fingertip force, stiffness and displacement, if the error between the virtual and the actual fingertip pose remains zero, F_n will not increase regardless of the change in k_n.

The above observations suggest that the implementation of a similar principle in a robotic or prosthetic hand to simultaneously and instantly regulate the virtual pose and the rigidity (stiffness) of the grasp can lead to a human-like grasping performance that ensures the grasp robustness against disturbances such as slippage.

III. Robotic Implementation

A. Experimental Setup

As previously mentioned, the main purpose of this study is to implement an appropriate and instantaneous grasp force regulation control law for the Pisa/IIT SoftHand [20] (Fig. 1. b). The goal of the SoftHand was to design and build a robotic hand that is highly functional yet simple and robust. This was achieved by combining the soft synergies approach with underactuation. The former uses human hand grasping synergies as a reference position for a virtual hand. The virtual hand position or stiffness profile connecting the virtual and real hands can thus be varied to control the

interaction forces between the hand and the environment. The latter employs fewer actuators than available degrees of freedom, thus lowering cost, weight, and complexity of the device. Underactuation also imparts a degree of adaptability to the hand, thus the combination of these techniques was termed "adaptive synergies". Additionally, to make the hand more robust and safer in human-robot interaction scenarios, the hand was designed with soft robotics principles in mind: the fingers can be bent, twisted, struck, etc., and will deform out of the way and then return to their original conformation, protecting both the hand and the environment from damage in the event of a collision. The SoftHand is anthropomorphic and contains a single motor. This motor pulls a tendon that winds through the fingers and thumb to simultaneously flex and abduct the fingers. Several studies have been performed to illustrate adaptive capabilities of the SoftHand together with a teleimpedance controller for grasping various objects with different elastic properties (e.g. see [21]). The hand unit and power driver of the SoftHand is a custom control board with the Tiva^{TM} TM4C123GH6PZ microcontroller (Texas Instruments). Motor current measurement is performed by a high side current sensing device (LT61081 by linear technologies) and appropriate signal conditioning integrated in the motor power driver module.

The setup incorporates a seven degrees-of-freedom KUKA lightweight robot, with DLR's Fast Research Interface. KUKA is programmed in Cartesian impedance control mode with relatively stiff components (with 1.5k $\frac{N}{m}$ translational and 100 $\frac{Nm}{rad}$ rotational) to avoid possible deviations from the desired Cartesian trajectories due to the unknown gravitational loading of the grasped objects. The SoftHand is mounted on the end-effector of KUKA using a custom made adaptor. Two ThimbleSense sensory units are integrated into the middle and thumb fingertips of the SoftHand, using an add-on on distal phalanxes to connect with the F/T sensor, thus obtaining contact point, force and torque measurements in the local finger reference frame (see Fig. 1). The placement of the ThimbleSense on the two fingertips will most likely provide the required data for the object slippage detection and control due to the SoftHand's grasping pattern. The data acquisition and synchronization between KUKA, SoftHand controllers and the ThimbleSense processing units are developed in C++.

Predefined Cartesian position trajectories were designed for the KUKA to move the SoftHand close to the target objects (Approach) and lift them (Lift-off) to a height of 15 cm above the initial location. This consideration was to produce consistent and repeatable Approach and Lift-off trajectories while comparing different reflex control modes. In some experiments, the KUKA robot was programmed to move the SoftHand in such a way that a ThimbleSense slides on the surface (along both translational and rotational directions) to identify the corresponding friction coefficient, prior to the Grasp (where the SoftHand's current controller is active, see section III-B) and Lift-off phases. Various objects with different surface properties (see Fig. 4) were utilized in our experiments to evaluate the grasp robustness against slippage.

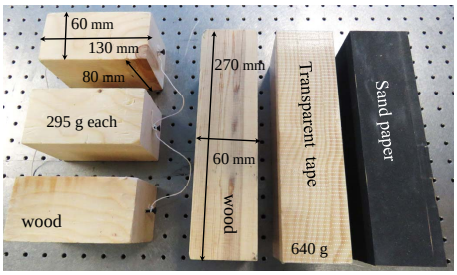

Fig. 4: Objects used in grasping experiments. Most left object emulates unexpected mass variations by interconnecting three blocks of wood using strings. The three objects on the right have different friction properties while being similar in shape and weight.

B. Control Architecture

Observations in human grasping experiments provide enough evidence on the necessity for the implementation of an instantaneous and appropriate grasp forces regulation mechanism to obtain a similar reflex behaviour in a robotic/prosthetic hand. A straightforward approach towards the achievement of this goal is direct control of the grasping forces by controlling the SoftHand's motor current profile. Alternatively, inspired by the human motor behaviour, interaction forces can be modulated by stiffening the hand and/or moving the virtual pose of the fingers into the object.

To explore the practical use of the above control concepts in our experimental setup, three reflex control modes, namely Current, Pose and Impedance are implemented and experimentally evaluated. In all three control modes, the grasping action (Grasp phase) is achieved by applying a feedforward term (I_{FF}, see Fig. 5) to the current controller of the SoftHand to move the hand fingers along the first human hand synergy reference. The underlying adaptive synergy concept of the SoftHand along with the implemented current controller provide flexibility in the grasp pattern and facilitate molding around the unknown object with a soft desired grasping force. This also ensures the establishment of a reliable contact between the ThimbleSenses' outer shells and the object's surface for reliable measurements of the tangential (F_t) and normal (F_n) forces and torques (τ) at the point of contact. This feature becomes even more advantageous when the SoftHand fingertip is sliding on the object's surface (Slide phase) for the estimation of the friction coefficient.

1) Detection: The procedure for the estimation of the static and dynamic values of the translational (μ_T) and rotational (μ_R) friction coefficients between two surfaces is long-recognized and fairly well-understood [8], [22]–[24]. As mentioned above, in our setup, this is achieved by sliding a fingertip ThimbleSense on the surface of the object using Cartesian KUKA trajectories. The peak values of $\frac{\|F_t\|}{\|F_n\|}$ and $\frac{\|\tau\|}{\|F_n\|}$ within the first 600 milliseconds of the Slide phase are detected and assumed as the object's translational and rotational friction coefficient, respectively.

Once the coefficients are known, the slippage detection can be achieved by monitoring the fingertip ThimbleSenses' data. For instance, in [25], a linear approximation of the

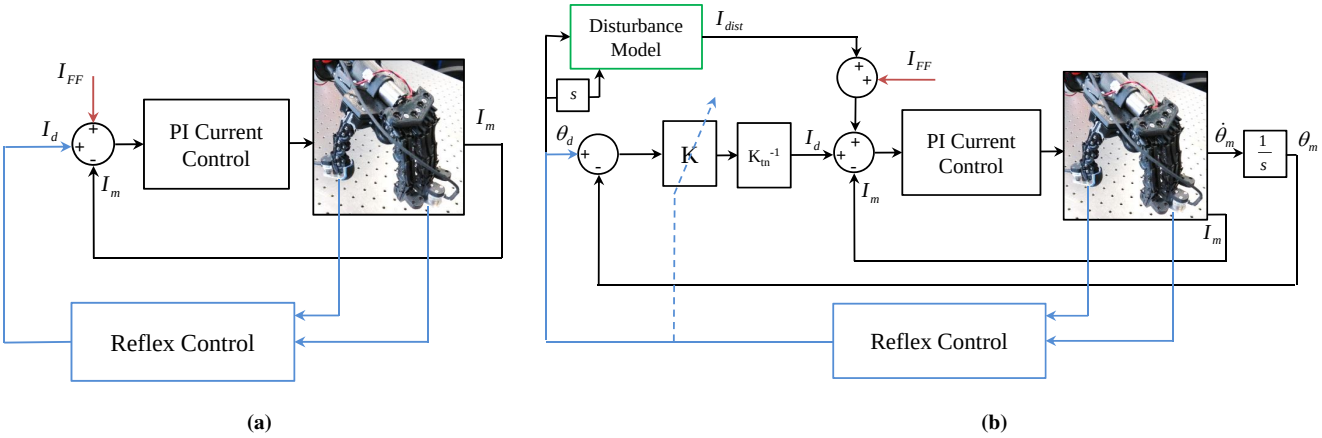

Fig. 5: Block diagrams of the three reflex control modes: a) Current reflex control, and b) Pose (excluding the dashed line) and Impedance (including the dashed line) reflex control. A feed-forward hand disturbance model is developed for enhanced tracking accuracy of the hand impedance controller (both Pose and Impedance modes) in low values of the K gain.

relationship between the forces and torques in a non-slippery contact is proposed as follows[3]

$$\frac{\|F_t\|}{\mu_{T_o}} + \frac{\|\tau\|}{\mu_{R_o}} \leq \|F_n\|, \tag{1}$$

with the index o referring to the static value of the friction coefficient, and $\|.\|$ denoting a vector norm. Accordingly, we define a slippage measure index for the thumb (S_1) and middle (S_3) fingers using acquired and processed fingertip data

$$S_{1,3} = \frac{\|F_{t_{1,3}}\|}{\mu_{T_o}} + \frac{\|\tau_{1,3}\|}{\mu_{R_o}} - \|F_{n_{1,3}}\|. \tag{2}$$

Positive values of either one of slippage measures (S_1 or S_3) correspond to the occurrence of the slippage. If both values are positive (or negative, when the grasp is firm), the worst case measure S_w is considered in the update laws of the implemented reflex control modes

$$S_w = \max\{S_1, S_3, 0\}. \tag{3}$$

2) Control: First reflex control mode (Fig. 5. a) implements a current control loop and updates the desired current as a function of the slippage measure index

$$\Delta I_d = c_F S_w, \tag{4}$$

in addition to the feed-forward term, I_{FF}, described above. The coefficient c_F is experimentally identified by taking into account the desired reflex speed. The advantage of using such an update law is that the reflex strength is regulated based on the slippage condition which is reflected by the S_w.

On the other hand, Pose and Impedance reflex control modes implement an impedance controller with an inner current control loop (see Fig. 5. b). The stiffness gain (K) in the Pose mode is considered a constant value while being regulated in Impedance mode once the object slippage is detected. In both modes, to enable a precise and accurate tracking of the hand trajectories in low values of the K gain, a feed-forward disturbance model of the hand is defined and experimentally identified. To achieve this, we write the equation of motor dynamics[4]

$$J_n \ddot{q} = K_{tn} I_{ref} - \tau_{DM}, \tag{5}$$

with $\ddot{q}$, K_{tn}, and I_{ref} denoting the motor angular acceleration, torque constant, and motor current, respectively. $J_n = J_m + \frac{J_h}{N^2}$ represents the total inertia (motor inertia plus hand and fingertip sensors' inertia reflected to the motor side).

In our setup, due to the low velocity profiles of the hand closure and the relatively high gear ratio, the reflected inertia of the hand, $\frac{J_h}{N^2}$, is neglected. The disturbance torque, τ_{DM}, is assumed to be formed by three components: the elastic torque generated by the hand tendons during closure (τ_{te}), the gravitational effect (τ_{grav}), and the frictional torque caused by the friction in the hand joints and pulleys (τ_f),

$$\tau_{DM} = \tau_{te} + \tau_f + \tau_{grav}. \tag{6}$$

Given the lightweight design of the SoftHand-ThimbleSense setup, we can safely neglect τ_{grav}. τ_{te} is modelled as a function of the motor shaft rotation angle. In addition, the viscous and Coulomb friction of the hand is modelled using an antisymmetric piecewise-linear function of the motor speed and tendon tension

$$\tau_f(\dot{q}) = \begin{cases} D_1\dot{q} + n_{s_1}K_{te}(q - q_o) & \dot{q} > 0 \\ D_2\dot{q} - n_{s_2}K_{te}(q - q_o) & \dot{q} < 0, \end{cases} \tag{7}$$

with D_i, n_{s_i}, K_{te}, and q_o representing the viscous damping and Coulomb friction coefficients, the reflected hand tendon stiffness, and motor angular position at rest (hand open),

[3]For a more complete discussion on the consideration of the contact area in rotational friction refer to [8].

[4]In this paper, all the variables and equations are described on the motor side. Therefore, a gearbox ratio of $N = 84$ must be taken into account for the presentation of the variables after the gearbox.

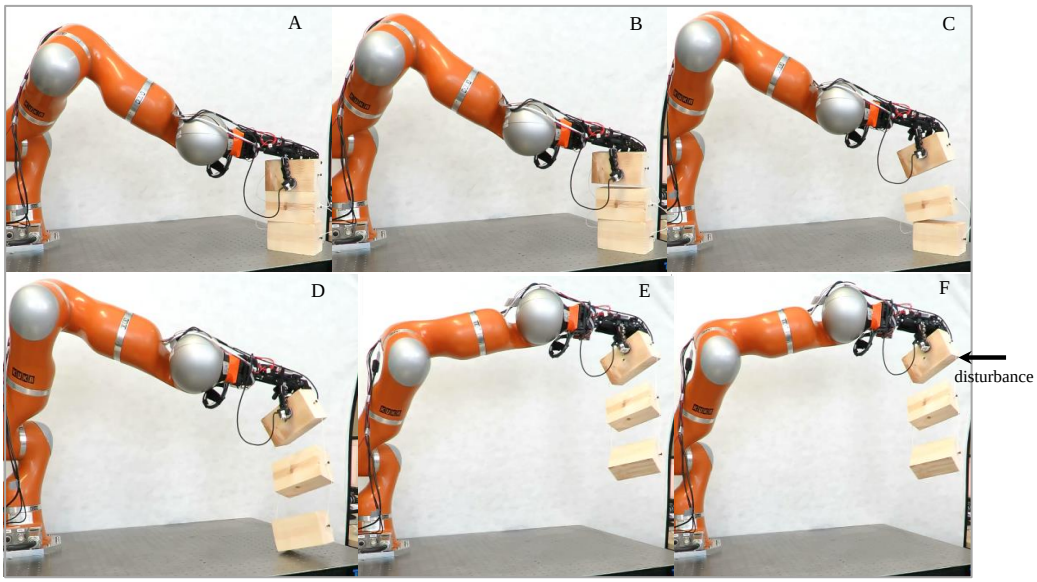

Fig. 6: Snapshots of the object lifting task with varying mass (A-E) and the applied external disturbance (F).

respectively. By integrating the above formulas we obtain

$$\tau_{DM} = \begin{cases} (1+n_{s_1})K_{te}(q-q_o)+D_1\dot{q} & \dot{q}>0 \\ (1-n_{s_2})K_{te}(q-q_o)+D_2\dot{q} & \dot{q}<0. \end{cases} \quad (8)$$

Supposing that the hand has not come in contact with the object to be grasped (therefore external forces are zero), the hand model torque (τ_{DM}) can be computed from the motor current and its motion response. Such calculation would require motor current and acceleration sensing with the latter being sensitive to noise if computed from position differentiation. To avoid this, we implement a robust torque observation technique for a reliable estimation of the hand model torque, as follows

$$\begin{aligned} \widehat{\tau}_{DM} &= K_{tn}I_{ref} - J_n\ddot{q} \\ \widehat{\tau}_{DM}(s) &\simeq \frac{\lambda}{s+\lambda}(K_{tn}I_{ref} - J_n s\dot{q}) \\ &\simeq \frac{\lambda}{s+\lambda}(K_{tn}I_{ref} + \lambda J_n\dot{q}) - \lambda J_n\dot{q}, \end{aligned} \quad (9)$$

with s being the Laplace operator and λ representing the filter cut-off frequency which defines the disturbance rejection capability [26]. The major design criterion is to choose λ low enough to result in a robust system, while considering the introduced filtering delay.

To identify the parameters of the hand model (equation 8), the hand controller was driven with fixed and low velocity (quasi-static) reference trajectories from the fully open to fully closed position. This process was repeated in the reverse direction as well, to account for the antisymmetric and velocity dependent properties of the friction model during opening and closure. Next, the resultant current, position, and velocity profiles were used to estimate the components of equation (8), by means of conventional least squares identification algorithm. The identification process led to two feed-forward, velocity dependent estimates of the hand disturbance model, $\widehat{\tau}_{DM}$.

Experimental evaluation of the identified hand model was performed by investigating the tracking accuracy of the hand controller with low values of the K gain. Consideration of the feed-forward term, for instance, led to %35 reduction of the mean absolute error (MAE) value while tracking a sine wave trajectory with the gain being set to $K = 5\frac{Nm}{rad}$ [5].

During Lift-off and once an slippage is detected, Pose reflex mode's update law regulates the SoftHand's grasp force by updating the hand closure reference

$$\Delta q_d = c_P S_w. \quad (10)$$

Whereas in Impedance reflex mode, hand closure trajectory and the stiffness gain are both adjusted as functions of the slippage measure[6]

$$\begin{aligned} \Delta q_d &= c_I S_w \\ \Delta K &= \bar{c}_I S_w. \end{aligned} \quad (11)$$

IV. Results

Even though a straightforward implementation of the grasp force regulation mechanism can result in a simpler and more compact representation of reflex feedback, it is well-known that such a control loop lacks robustness since force (current) measurements are subject to noise and drift. In particular, when an instantaneous force reflex is required in response to the object slippage, such noise can cause oscillations in the motor current and generate a non-smooth interaction force, as a consequence[7]. This behaviour can be observed in Fig.

[5]For a detailed analysis of the hand disturbance model, please see [27].

[6]Coefficients c_P, c_I, and $\bar{c}_I$ are experimentally identified based o the desired reflex speed.

[7]Filtering of the motor current can resolve the problem up to some extent, however, this will introduce delays in the control loop which affects reflexive capabilities of the controller.

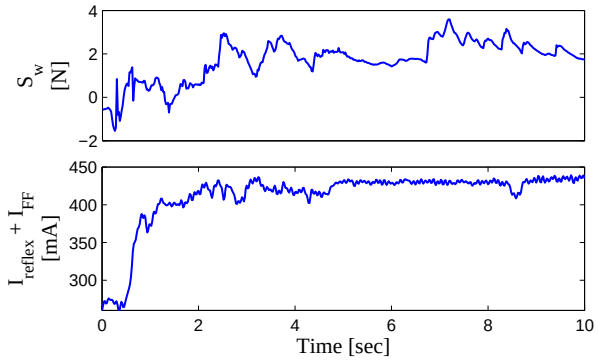

Fig. 7: Experimental results of the Current reflex controller during Lift-off phase of an object with the varying mass. Sudden mass variations cause slippage and require that the motor current profile is instantaneously adjusted. Nonetheless, due to the sensitivity of the current sensing and control to noise, potential oscillations can be generated in the motor current and the contact force profile, as a consequence. This may cause undesired oscillatory movements of the object that will affect S_W (can be seen from $t = 7s$) and might lead to the grasp failure.

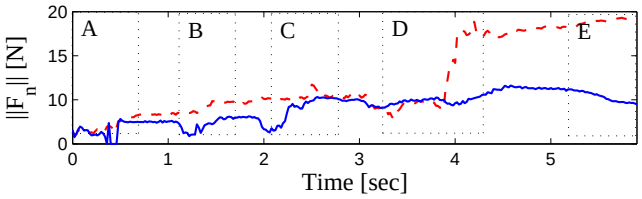

Fig. 8: Experimental results of the Pose (red, dashed) and Impedance (blue, solid) reflex modes for picking a test object. Different phases of the task are labelled by characters A to E which correspond to the snapshots of the experiment in Fig. 6.

7, in which the SoftHand was picking up the test object with varying mass (Fig. 4, most left).

Fig. 6 (A-E) illustrates the snapshots of an experiment in which the Pose and the Impedance reflex control modes were applied while lifting the same object. Both modes demonstrated robustness against slippage, however, Pose generated higher normal forces compared to the case in which both position and stiffness gains were gradually modulated in response to the object slippage (see Fig. 8)[8].

Fig. 9 shows typical results of a similar experiment where the Impedance reflex mode is operating on the SoftHand control board to realize a robust grasp against varying load (blocks A-E) and external disturbance (block F which correspond to Fig. 6-F). As depicted in the plots, the virtual grasp pose and stiffness parameter are appropriately regulated to realize a firm grasp while avoiding non-smooth or unnecessary high interaction forces (a video of the experiment is available at [28]). This behaviour is consistent with the observations in our human grasping experiments (see Fig. 2) which suggest that the grasp pose and stiffness are synchronously regulated in humans to establish a reliable contact between the object and the fingers. Implementation of a similar control principle in prosthetic applications of the SoftHand will result in intuitive regulation of the stiffness gain and pose references, and if necessary, will be finely tuned by the reflex controller.

[8]To provide a simple explanation, consider that the Impedance reflex mode is implemented in such a way to achieve a minimum-required grasping force profile in response to the worst case object slippage S^*_w, by generating stiffness δk and position δq increments. The interaction force increment therefore will approximately be $\delta F \approx (k+\delta k)(\delta q)$. Now imagine that the Pose controller's gain is pre-set to $k+\delta k$. To achieve a similar interaction force, c_P must be chosen in such a way that $\Delta q_d = \delta q$. Now if the slippage index becomes smaller, for instance $\frac{S^*_w}{b}$, Impedance and Pose will generate $(k+\frac{\delta k}{b})(\frac{\delta q}{b})$, and $(k+\delta k)(\frac{\delta q}{b})$, respectively. This example illustrates that Pose interaction forces will be higher than Impedance, unless the update gains are non-constant.

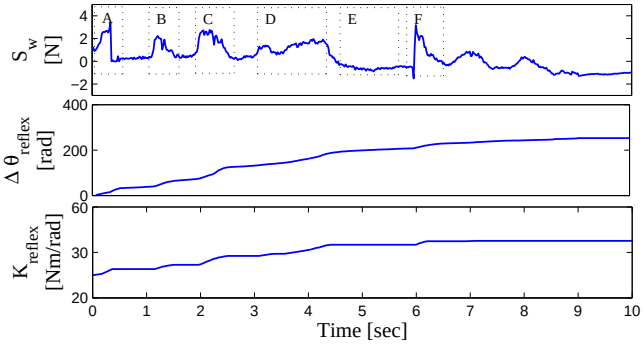

Fig. 9: Experimental results of the Impedance reflex during Lift-off (varying mass (A-E) and external disturbance (F)). Impedance reflex mode regulated the grasp forces by updating the grasping pose (q) and stiffness (K) so that disturbances (mass variations or external) do not cause slippage.

To further evaluate the efficacy of the proposed Impedance reflex controller, objects which only differ in surface properties (three most-right objects in Fig. 4) were considered in our experimental trials. First, friction coefficients of the objects were estimated in the Slide phase and exploited by the Impedance reflex controller. Consequently, the objects were grasped using the feed-forward term (I_{FF}) and lifted to a constant height. I_{FF} was set to be just enough to pick the object with the sandpaper surface. As a result, the Impedance reflex did not generate unnecessary additional forces to stabilise this object during Lift-off (Fig. 10, red plots). On the other hand, task-efficient restoring forces were applied to avoid slippage while picking the objects with wood (blue plots) and tape (green plots) surfaces.

V. Conclusions

In this work, with the aim to establish a reliable contact between the SoftHand and the object during grasping, three reflex control modes were implemented and experimentally compared. Proposed controllers regulated the restoring grasp forces by updating the motor current profile (Current), grasp pose (Pose) and stiffness (Impedance) once the slippage is detected. Real-time detection and control of the slippage was established by defining an index measure using two fingertip ThimbleSense data. Results suggested that the Impedance reflex mode generated instantaneous and human-like reflexive response to avoid the slippage, highlighting its potential for prosthetic applications of the SoftHand-ThimbleSense setup. Future research will explore the robustness and the

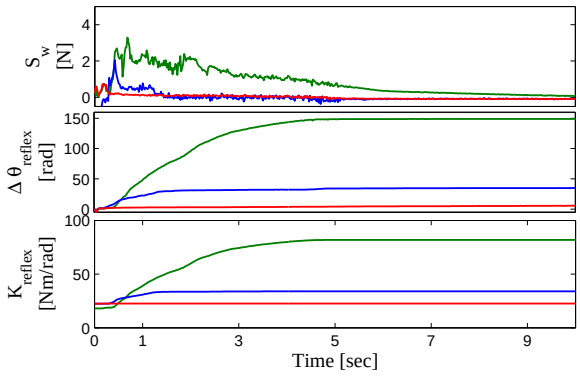

Fig. 10: Typical results of an experiment in which objects with different surface properties (transparent tape (green), wood (blue), and sandpaper (red)) are grasped and lifted. Impedance reflex controller effectively regulated the grasp posture (middle plot) and stiffness (bottom plot), in response to the slippage measure (upper plot).

stability of the proposed reflex controller for grasping highly deformable objects.

REFERENCES

[1] J. Johansson, R. S.and Flanagan, *Tactile sensory control of object manipulation in humans*. Elsevier, 2007, vol. 6, ch. Handbook of the Senses.

[2] C. Cipriani, F. Zaccone, S. Micera, and M. C. Carrozza, "On the shared control of an emg-controlled prosthetic hand: analysis of user–prosthesis interaction," *Robotics, IEEE Transactions on*, vol. 24, no. 1, pp. 170–184, 2008.

[3] Touch Bionics Inc., 2015. [Online]. Available: Available:http://www.touchbionics.com/products/active-prostheses/i-limb-ultra/

[4] M. Tremblay and M. Cutkosky, "Estimating friction using incipient slip sensing during a manipulation task," in *IEEE International Conference on Robotics and Automation*, vol. 1, May 1993, pp. 429–434.

[5] L. Roberts, G. Singhal, and R. Kaliki, "Slip detection and grip adjustment using optical tracking in prosthetic hands," in *IEEE EMBC International Conference on Engineering in Medicine and Biology Society*, Aug 2011, pp. 2929–2932.

[6] G. Canepa, R. Petrigliano, M. Campanella, and D. De Rossi, "Detection of incipient object slippage by skin-like sensing and neural network processing," *IEEE Transactions on Systems, Man, and Cybernetics, Part B: Cybernetics*, vol. 28, no. 3, pp. 348–356, Jun 1998.

[7] C. Bauer, G. Milighetti, W. Yan, and R. Mikut, "Human-like reflexes for robotic manipulation using leaky integrate-and-fire neurons," in *IEEE/RSJ International Conference on Intelligent Robots and Systems (IROS)*, Oct 2010, pp. 2572–2577.

[8] C. Melchiorri, "Slip detection and control using tactile and force sensors," *Mechatronics, IEEE/ASME Transactions on*, vol. 5, no. 3, pp. 235–243, 2000.

[9] G. Johansson, R. S.and Westling, "Tactile afferent signals in the control of precision grip," 1990, pp. 677–713.

[10] J. Fishel, V. Santos, and G. Loeb, "A robust micro-vibration sensor for biomimetic fingertips," in *IEEE RAS EMBS International Conference on Biomedical Robotics and Biomechatronics (BioRob)*, Oct 2008, pp. 659–663.

[11] T. Mouri, H. Kawasaki, and S. Ito, "Unknown object grasping strategy imitating human grasping reflex for anthropomorphic robot hand," *Journal of Advanced Mechanical Design, Systems, and Manufacturing*, vol. 1, no. 1, pp. 1–11, 2007.

[12] H. Yussof and M. Ohka, "Application of stiffness control algorithm for dexterous robot grasping using optical three-axis tactile sensor system," in *Micro-NanoMechatronics and Human Science, 2009. MHS 2009. International Symposium on*. IEEE, 2009, pp. 472–476.

[13] H. Soma, Y. Horiuchi, J. Gonzalez, and W. Yu, "A study on the forearm muscular reflexes during grasping for prosthetic applications," in *Annual International Conference of the IEEE Engineering in Medicine and Biology Society (EMBC)*. IEEE, Aug 2010, pp. 4886–4889.

[14] I. Kao, M. R. Cutkosky, and R. S. Johansson, "Robotic stiffness control and calibration as applied to human grasping tasks," *Robotics and Automation, IEEE Transactions on*, vol. 13, no. 4, pp. 557–566, 1997.

[15] H.-Y. Han and S. Kawamura, "Analysis of stiffness of human fingertip and comparison with artificial fingers," in *Systems, Man, and Cybernetics, 1999. IEEE SMC'99 Conference Proceedings. 1999 IEEE International Conference on*, vol. 2. IEEE, 1999, pp. 800–805.

[16] E. Battaglia, G. Grioli, M. G. Catalano, M. Santello, and A. Bicchi, "Thimblesense: an individual-digit wearable tactile sensor for experimental grasp studies," in *Proceedings of IEEE International Conference on Robotics and Automation*, 2014.

[17] A. Bicchi, J. K. Salisbury, and D. L. Brock, "Contact sensing from force measurement," *The International Journal of Robotics Research*, vol. 12, pp. 249–262, 1993.

[18] A. Serio, E. Riccomini, V. Tartaglia, I. Sarakoglou, M. Gabiccini, N. Tsagarakis, and A. Bicchi, "The patched intrinsic tactile object: A tool to investigate human grasps," in *Intelligent Robots and Systems (IROS 2014), 2014 IEEE/RSJ International Conference on*, Sept 2014, pp. 1261–1268.

[19] D. W. Franklin, R. Osu, E. Burdet, M. Kawato, and T. E. Milner, "Adaptation to stable and unstable dynamics achieved by combined impedance control and inverse dynamics model," *Journal of neurophysiology*, vol. 90, no. 5, pp. 3270–3282, 2003.

[20] M. G. Catalano, G. Grioli, E. Farnioli, A. Serio, C. Piazza, and A. Bicchi, "Adaptive synergies for the design and control of the pisa/iit softhand," *The International Journal of Robotics Research*, vol. 33, no. 5, pp. 768–782, 2014.

[21] A. Ajoudani, S. Godfrey, M. Bianchi, M. Catalano, G. Grioli, N. Tsagarakis, and A. Bicchi, "Exploring teleimpedance and tactile feedback for intuitive control of the Pisa/IIT softhand," *IEEE Transactions on Haptics*, vol. 7, pp. 203–2015, 2014.

[22] M. R. Cutkosky and P. K. Wright, "Friction, stability and the design of robotic fingers," *The International Journal of Robotics Research*, vol. 5, no. 4, pp. 20–37, 1986.

[23] A. Bicchi, J. Salisbury, and D. Brock, "Experimental evaluation of friction data with an articulated hand and intrinsic contact sensors," *Experimental robotics: III (eds Chatila R., Hirzinger G.), Berlin/Heidelberg, Germany: Springer*, 1993.

[24] N. Xydas and I. Kao, "Modeling of contact mechanics and friction limit surfaces for soft fingers in robotics, with experimental results," *The International Journal of Robotics Research*, vol. 18, no. 9, pp. 941–950, 1999.

[25] R. D. Howe, I. Kao, and M. R. Cutkosky, "The sliding of robot fingers under combined torsion and shear loading," in *Robotics and Automation, 1988. Proceedings., 1988 IEEE International Conference on*. IEEE, 1988, pp. 103–105.

[26] T. Murakami, F. Yu, and K. Ohnishi, "Torque sensorless control in multidegree-of-freedom manipulator," *Industrial Electronics, IEEE Transactions on*, vol. 40, no. 2, pp. 259–265, 1993.

[27] A. Ajoudani, S. B. Godfrey, M. Catalano, G. Grioli, N. G. Tsagarakis, and A. Bicchi, "Teleimpedance control of a synergy-driven anthropomorphic hand," in *Intelligent Robots and Systems (IROS), 2013 IEEE/RSJ International Conference on*. IEEE, 2013, pp. 1985–1991.

[28] http://youtu.be/8Q33gKBQ5ok.